Proceedings of ICAR 2003
The 11th International Conference on Advanced Robotics
Coimbra, Portugal, June 30 - July 3, 2003

Non Linear Lateral Control of Vision Driven Autonomous Vehicles

Miguel Angel Sotelo

Department of Electronics. University of Alcala.
Campus Universitario s/n. Alcala de Henares. 28871. Madrid. Spain.
michael@depeca.uah.es

Abstract

This paper presents the results of a lateral control strategy that has been applied to the problem of steering an autonomous vehicle using vision. The lateral control law has been designed for any kind of car-like vehicle presenting the Ackerman kinematic model, accounting for the vehicle velocity as a crucial parameter for adapting the steering control response. This makes the control strategy suitable for either low or high speed vehicles. The stability of the control law has been analitically proved, and experimentally tested by autonomously steering Babieca, a Citroen Berlingo prototype vehicle.

1 Introduction

Lateral automatic steering of autonomous car-like vehicles has become an apparent field of application for robotics researchers. Basically, this problem can be stated as that of determining an appropriate control law for commanding the vehicle steering angle. Many steering control designs are already documented in the literature [1], [3]. A comparative study on various lateral control strategies for autonomous vehicles can be found in [11], where a linearized model of the lateral vehicle dynamics is used for controller design basing on the fact that it is possible to decouple the longitudinal and lateral dynamics. On the contrary, a simplified non linear lateral kinematic model is proposed in this work, intended to ease the design and implementation of a stable lateral control law for autonomous steering of car-like vehicles. The lateral control strategy was implemented on Babieca, an electric Citroen Berlingo experimental prototype, using vision as the main sensor to measure the position of the vehicle in the road. Real tests were carried out on a private circuit emulating an urban quarter, composed of streets, intersections (crossroads), and roundabouts, located at the Industrial Automation Institute (IAI) in Arganda del Rey, Madrid. Additionally, a live demonstration exhibiting the system capacities on autonomous steering was carried out during the IEEE Conference on Intelligent Vehicles 2002, in a private circuit located at Satory (Versailles), France.

2 Lateral Control

Considering the case of an autonomous vehicle driving along some reference trajectory, the main goal of the lateral control module is to ensure proper tracking of the reference trajectory by correctly keeping the vehicle in the center of the lane with the appropriate orientation (parallel to the desired trajectory). This constraint can be generalized as the minimization of the vehicle lateral and orientation errors (d_e,θ_e) with respect to the reference trajectory, at a given distance L_h denoted by Look-ahead distance, as illustrated in figure 1. To solve this controllability problem and design a stable lateral controller, a model describing the dynamic behaviour of d_e and θ_e is needed.

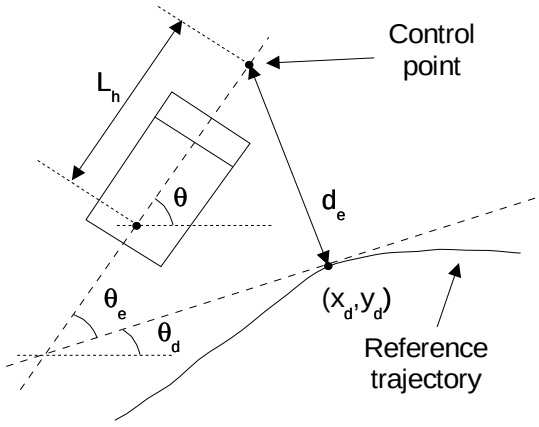

Figure 1: *Lateral and orientation errors at the Look-ahead distance.*

2.1 Kinematic model

The kinematic model of the vehicle is the starting point to model the dynamics of the lateral and orientation errors. The vehicle model is approximated by the popular Ackerman (or bicycle) model [4] as depicted in figure 2, assuming that the two front wheels turn slightly differentially and thus, the instantaneous

rotation center can be purely computed by kinematic means. Let $\kappa(t)$ denote the instantaneous curvature of the trajectory described by the vehicle.

$$\kappa(t) = \frac{1}{R(t)} = \frac{\tan\phi(t)}{L} = \frac{d\theta(t)}{ds} \quad (1)$$

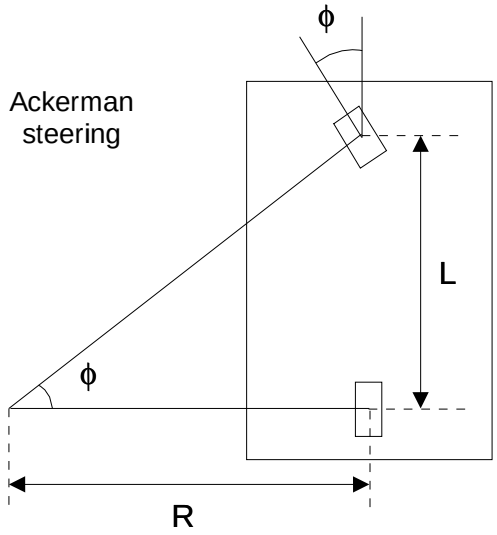

Figure 2: *Approximate kinematic model of the vehicle (Ackerman steering).*

where R is the radius of curvature, L is the wheelbase, ϕ is the steering angle, and θ stands for the vehicle orientation in a global frame of coordinates. The dynamics of θ are computed in equation 2 as a function of vehicle velocity v.

$$\dot{\theta} = \frac{d\theta}{dt} = \frac{d\theta}{ds} \cdot \frac{ds}{dt} = \kappa(t) \cdot v(t) = \frac{\tan\phi(t)}{L} \cdot v(t) \quad (2)$$

Let ϕ and v be the variables of the vehicle actuation space. On the other hand, the vehicle configuration space is composed of the global position and orientation variables, described by (x, y, θ), under the flat terrain assumption. Mapping from the actuation space to the configuration space can be solved by using the popular Fresnel equations, which are also the so-called dead reckoning equations typically used in inertial navigation. Equation 3 shows the dynamics of (x, y, θ).

$$\begin{aligned} \dot{x} &= \tfrac{dx}{dt} = v(t)\cos\theta(t) \\ \dot{y} &= \tfrac{dy}{dt} = v(t)\sin\theta(t) \\ \dot{\theta} &= \tfrac{d\theta}{dt} = v(t)\tfrac{\tan\phi(t)}{L} \end{aligned} \quad (3)$$

where $v(t)$ represents the velocity of the midpoint of the vehicle rear axle. Global information about the position and orientation of the vehicle (x, y, θ) is then transformed so as to develop a model that describes the open-loop lateral and orientation error dynamics.

As observed in figure 1, the lateral error d_e is defined as the distance between the vehicle control point, located at the Look-ahead distance, and the closest point along the vehicle desired trajectory, described by coordinates (x_d, y_d). This implies that d_e is perpendicular to the tangent to the reference trajectory at (x_d, y_d). The scope of the tangent at (x_d, y_d) is denoted by θ_d, and represents the desired orientation at that point. Basing on this, d_e and θ_e suffice to precisely characterize the location error between the vehicle and some given reference trajectory, as described in equation 4.

$$\begin{aligned} d_e = &-(x + L_h\cos\theta - x_d)\sin\theta_d \\ &+(y + L_h\sin\theta_d - y_d)\cos\theta_d \\ \theta_e = &\ \theta - \theta_d \end{aligned} \quad (4)$$

The choice of L_h is carried out basing on the current vehicle velocity v, as described in [2], yielding the parameters shown in equation 5.

$$L_h(v) = \begin{cases} L_{min} & if \quad v < v_{min} \\ v \cdot t_1 & if \quad v_{min} \le v \le v_{max} \\ L_{max} & if \quad v > v_{max} \end{cases} \quad (5)$$

where $t_1 = 1.5s$ is the Look-ahead time, $v_{min} = 25km/h$, $v_{max} = 75km/h$, $L_{min} = 10.41m$, and $L_{max} = 31.25m$. Computing the derivatives of d_e and θ_e with respect to time yields the complete non linear model described in equation 6.

$$\begin{aligned} \dot{d}_e &= v\sin\theta_e + \tfrac{vL_h}{L}\cos\theta_e\tan\phi \\ \dot{\theta}_e &= \tfrac{v\tan\phi}{L} \end{aligned} \quad (6)$$

2.2 Non linear control law

The control objective is to ensure that the vehicle will correctly track the reference trajectory. For this purpose, both the lateral error d_e and the orientation error θ_e must be minimized. On the other hand, vehicle velocity v will be assumed to be constant, for simplicity. The design of the control law is based on general results in the so-called chained systems theory [8]. Excellent examples on this topic can be found in [5], [7]. Nevertheless, these results are extended and generalized in this paper so as to provide a stable non linear control law for steering of car-like vehicles basing on local errors. From the control point of view, the use of the popular tangent linearization approach is avoided as it is only valid locally around the configuration chosen to perform the linearization, and thus, the initial conditions may be far away from the reference trajectory. On the contrary, some state and control variables changes are posed in order to convert the non linear system described in equation

6 into a linear one, without any approximation (exact linearization approach). Nevertheless, due to the impossibility of exactly linearizing systems describing mobile robots dynamics, these non linear systems can be converted in almost linear ones, termed as chained form. The use of the chained form permits to design a control law using linear systems theory to a high extent. In particular, the non linear model for d_e and θ_e (equation 6) can be transformed into chained form using the state diffeomorphism and change of control variables, as in equation 7.

$$Y = \begin{bmatrix} y_1 \\ y_2 \end{bmatrix} = \Theta(X) = \begin{bmatrix} d_e \\ \tan\theta_e \end{bmatrix}$$
$$W = \begin{bmatrix} w_1 \\ w_2 \end{bmatrix} = \Upsilon(U) = \begin{bmatrix} v\cos\theta_e + \frac{vL_h\cos^2\theta_e\tan\phi}{L\sin\theta_e} \\ \frac{v\tan\phi}{L\cos^2\theta_e} \end{bmatrix} \tag{7}$$

These transformations are invertible whenever the vehicle speed v is different from zero, and the orientation error θ_e is different from $\frac{\pi}{2}$. This implies that the singularities of the transformations can be avoided by assuring that the vehicle moves ($v > 0$) and that its orientation error is maintained under 90 degrees (the vehicle orientation must not be perpendicular to the reference trajectory). These conditions are reasonably simple to meet in practice. From equation 7 the vehicle model can be rewritten as in equation 8, considering y_1 and y_2 as the new state variables.

$$\begin{aligned} \dot{y}_1 = \dot{d}_e &= v\sin\theta_e + \tfrac{vL_h}{L}\cos\theta_e\tan\phi = w_1 y_2 \\ \dot{y}_2 = \tfrac{d(\tan\theta_e)}{dt} &= \tfrac{1}{\cos^2\theta_e}\cdot\dot{\theta}_e = \tfrac{v\tan\phi}{L\cos^2\theta_e} = w_2 \end{aligned} \tag{8}$$

In order to get a velocity independent control law, the time derivative is replaced by a derivation with respect to ς, a variable related to the abscissa along the tangent to the reference trajectory. Analytically, ς is computed according to the following expression.

$$\varsigma = \int (v\cos\theta_e + \frac{vL_h\cos^2\theta_e\tan\phi}{L\sin\theta_e})\cdot dt \tag{9}$$

The time derivative of the state variables y_1 and y_2 is expressed as a function of ς in equation 10.

$$\begin{aligned} \dot{y}_1 &= \tfrac{dy_1}{dt} = \tfrac{dy_1}{d\varsigma}\cdot\tfrac{d\varsigma}{dt} = y_1^{'}\cdot\dot{\varsigma} \\ \dot{y}_2 &= \tfrac{dy_2}{dt} = \tfrac{dy_2}{d\varsigma}\cdot\tfrac{d\varsigma}{dt} = y_2^{'}\cdot\dot{\varsigma} \end{aligned} \tag{10}$$

where y_1' and y_2' stand for the derivative of y_1 and y_2 with respect to ς, respectively. Solving for y_1' and y_2' yields to equation 11.

$$\begin{aligned} y_1^{'} &= \tan\theta_e = y_2 \\ y_2^{'} &= \frac{\tan\phi}{L\cos^3\theta_e + L_h\frac{\cos^4\theta_e\tan\phi}{\sin\theta_e}} = w_3 \end{aligned} \tag{11}$$

As observed in the previous equation, the transformed system is linear and thus, state variables y_1 and y_2 can be regulated to zero (so as to yield $d_e = d_{e,ref} = 0$ and $\theta_e = \theta_{e,ref} = 0$) by using the control low proposed in equation 12.

$$w_3 = -K_d y_2 - K_p y_1 \qquad (K_d, K_p) \in \Re^{+2} \tag{12}$$

Using equations 11 and 12 and solving for variable y_1 yields to equation 13, where the dynamic behaviour of y_1 with respect to ς is demonstrated to be linear.

$$y_1^{''} + K_d y_1^{'} + K_p y_1 = 0 \tag{13}$$

This implies that variables $y_1(= d_e)$ and $y_2(= \tan\theta_e)$ tend to zero as variable ς grows. The previous statement is analytically expressed in equation 14.

$$\lim_{\varsigma\to\infty} d_e = \lim_{\varsigma\to\infty} \theta_e = 0 \tag{14}$$

Accordingly, variable ς must always grow so as to ensure that both d_e and θ_e tend to zero. This condition is met whenever $v > 0$ and $-\pi/2 < \theta_e < \pi/2$. In other words, the vehicle must continuously move forward and the absolute value of its orientation error should be below $\pi/2$ in order to guarantee proper trajectory tracking. Thus, the non linear control law is finally derived from equations 11 and 12.

$$\phi = \arctan\left[\frac{-L\sin\theta_e\cos^3\theta_e(K_d\tan\theta_e + K_p d_e)}{\sin\theta_e + L_h\cos^4\theta_e(K_d\tan\theta_e + K_p d_e)}\right] \tag{15}$$

The control law is then modified by a sigmoidal function so as to account for physical limitations in the vehicle wheels turning angle and prevent from actuator saturation. On the other hand, the use of sigmoidal functions preserves the system stability as demonstrated in [10]. From observation of equation 13, the dynamic response of variable y_1 can be considered to be a second order linear one. In practice, it is not indeed linear due to the sigmoidal function used to saturate the control law, although it can be reasonably approximated as such. Thus, an analogy between constants K_d , K_p, and the parameters of a second order linear system ξ (damping coefficient) and ω_n (natural frequency) can be established, yielding equation 16.

$$\begin{aligned} \omega_n &= \sqrt{K_p} \\ \xi &= \frac{K_d}{2\sqrt{K_p}} \end{aligned} \tag{16}$$

Likewise, system overshoot M_p and settling distance d_s (given that the system error dynamics are described as a function of space variable ς, not time) can be obtained from equation 17.

$$\begin{aligned} M_p &= \exp^{\frac{-\xi\pi}{\sqrt{1-\xi^2}}} \\ d_{s|2\%} &= \frac{4}{\xi\omega_n} \end{aligned} \tag{17}$$

The design of constants K_d and K_p is undertaken considering that the system overshoot must not exceed 10% of the step input, and that the settling distance should be below some given threshold. Thus, for a typical settling time $t_s = 20s$, and given the vehicle velocity v, the proper settling distance can be computed as in equation 18.

$$d_s = t_s \cdot v = 20v \tag{18}$$

The value of K_d is derived from equations 16 and 17 yielding the velocity dependant expression in equation 19.

$$K_d = \frac{8}{d_s} = \frac{0.4}{v} \tag{19}$$

Likewise, dumping coefficient ξ is derived from equations 16 and 17, as shown in equation 20.

$$\xi = \sqrt{\frac{1}{\left[\frac{\pi}{\ln 0.1}\right]^2 + 1}} = \frac{K_d}{2\sqrt{K_p}} = \frac{4}{d_s\sqrt{K_p}} \tag{20}$$

Finally, K_p is deduced from the previous equation, yielding equation 21.

$$K_p = \left[\frac{6.766}{d_s}\right]^2 = \left[\frac{0.3383}{v}\right]^2 \tag{21}$$

The dependence of K_p and K_d on vehicle velocity v permits to ensure proper dynamic response. In particular, vehicle turning angle will be soft at high speeds, therefore avoiding possible oscillations due to physical constraints in steering dynamics.

3 Implementation and Results

The control law for autonomous steering described in this paper was tested on the so-called Babieca prototype vehicle (an electric Citroen Berlingo), as depicted in figure 3. The vehicle was modified to allow for automatic velocity and steering control at a maximum speed of 90 km/h. Babieca is equipped with a colour camera, to provide lateral and orientation position of the ego-vehicle with regard to the center of the lane, a Pentium PC, and a set of electronic devices to provide actuation over the accelerator and steering wheel, as well as to encode the vehicle velocity and steering angle. The colour camera provides standard PAL video signal at 25 Hz that is processed by a Meteor frame grabber installed on a 120 MHz Pentium running the Real Time Linux operating system. The complete navigation system, implemented under Real Time Linux using a pre-emptive scheduler, runs a vision-based lane tracking task for computing the lateral and orientation errors, as described in [14].

Practical experiments were conducted on a private circuit located at the Industrial Automation Institute

Figure 3: *Babieca prototype vehicle.*

in Arganda del Rey (Madrid). The circuit is composed of several streets, intersections, and roundabout points, trying to emulate an urban quarter. Various practical trials were conducted so as to test the validity of the control law for different initial conditions in real circumstances. During the tests, the reference vehicle velocity is kept constant by a velocity controller. Coefficients K_d and K_p were calculated as a function of v using equations 19 and 21. Figures 4 and 5 show the transient response of the vehicle lateral and orientation errors for reference velocities of 20 km/h, and 50 km/h, respectively. In both cases, the vehicle starts the run at an initial lateral error of about 1m, and an initial orientation error in the range $\pm 5°$. As can be clearly appreciated, the steady state response of the system is satisfactory for either experiments. Thus, the lateral error is bound to $\pm 5cm$ at low speeds and $\pm 25cm$ at v=50 km/h, while the absolute orientation error in steady state remains below $1°$ in all cases. Just to give an example on how the practical results conform to the expected values as derived from the theoretical development, let's consider the transient response of the vehicle depicted in figure 4 for v=20 km/h. Assuming a theoretical maximum overshoot of $M_p = 10\%$ and a settling time of $t_s = 20s$, the controller coefficients are tuned to $K_d = 0.072$ and $K_p = 0.0037$, according to equations 19 and 21. Nonetheless, from observation of figure 4 the maximum overshoot obtained in practice yields up to almost 25% for both the lateral and orientation errors, while the settling time takes some 22s. This is mainly due to the existence of non linear actuator dynamics and latencies, not considered in the model. In spite of these slight differences with regard to the theoretical expected values, the practical results exhibited in this section demonstrate that the non linear lateral control law developed in this work still permits to safely steer the vehicle at operational velocities.

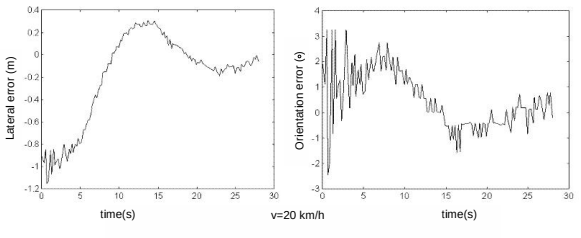

Figure 4: *Transient response of the lateral and orientation error for v=20 km/h.*

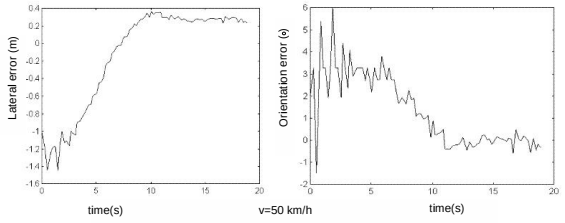

Figure 5: *Transient response of the lateral and orientation error for v=50 km/h.*

In a final trial, the results achieved in the second test for v=20 km/h are compared to human driving at the same speed along the same trajectory. For this purpose a human driver steered the vehicle, leaving the control of the accelerator to the velocity controller in order to keep a reference speed of 20 km/h. The comparison is graphically depicted in figure 6.

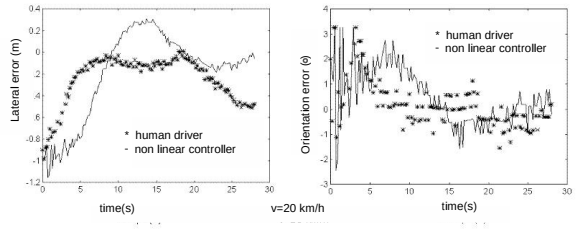

Figure 6: *Comparison between automatic guidance and human driving at v=20 km/h.*

On one hand, one can observe how the human driver takes less time than the automatic controller to achieve lateral and orientation errors close to zero. On the other hand, the steady state errors are similar in both cases. Surprisingly, human driving turns out in sporadic separations from the reference trajectory up to 40-50 cm, without incurring in dangerous behaviour, while the automatic controller keeps the vehicle under lower lateral error values once stabilized. Far from being an isolated fact, this circumstance was repeatedly observed in several practical experiments. As conclusion, the lateral control law developed in this work can reasonably be considered to be valid to drive a car-like vehicle as precisely as a human can. During the last year, Babieca ran over hundreds of kilometers in lots of successful autonomous missions carried out along the test circuit using the non linear control law described in this paper. A live demonstration exhibiting the system capacities on autonomous driving using the non linear control law described in this paper was carried out during the IEEE Conference on Intelligent Vehicles 2002, in a private circuit located at Satory (Versailles), France. A complete set of video files demonstrating the operational performance of the control system in real test circuits (both in Arganda del Rey and in Satory) can be retrieved from ftp://www.depeca.uah.es/pub/vision.

4 Conclusions

To conclude, the next key points should be remarked.

- First of all, the non linear control law described in this work has proved its analytical and empirical stability for lateral driving of car-like vehicles. In fact, it has been implemented on a real commercial vehicle slightly modified so as to allow for autonomous operation, and tested on two different private circuits.
- Vehicle commanded actuation is taken into account by considering the current velocity in the design of the controller coefficients. This permits to adapt the steering angle as a function of driving conditions.
- As demonstrated in practical trials, driving precision achieved by the lateral control law is as accurate as that of a human driver under normal conditions.

Nonetheless, in spite of having achieved some promising results there is still much space for improvement concerning vehicle stability and oscillations. Indeed, our current work focuses on accounting for more precise vehicle models including actuator dynamics and non linearities. Accordingly, a new non linear control law should be developed in an attempt to increase stability and comfortability when driving at high speed.

Acknowledgements

This work has been funded by the Department of Electronics of the UAH (*Universidad de Alcalá*), and

the generous support of the Industrial Automation Institute of the CSIC (*Consejo Superior de Investigaciones Cientificas*).

References

[1] J. Ackermann and W. Sienel, "Robust control for automated steering", in *Proc. of the 1990 American Control Conference, ACC90*, pp. 795-800, San Diego, CA, 1990.

[2] A. Broggi, M. Bertozzi, A. Fascioli, and G. Conte. *Automatic Vehicle Guidance: the Experience of the ARGO Autonomous Vehicle*. World Scientific. 1999.

[3] R. H. Byrne, C. T. Abdallah, and P. Dorato. "Experimental results in robust lateral control of highway vehicles", *IEEE Control Systems* 18(2), pp. 70-76, 1998.

[4] S. Cameron and P. Proberdt. *Advanced Guided Vehicles. Aspects of the Oxford AGV Project*. Ed. by World Scientific Publishing Co. Pte. Ltd. 1994.

[5] L. Cordesses, P. Martinet, B. Thuilot, and M. Berducat. "GPS-based control of a land vehicle". *IAARC/IFAC/IEEE International Symposium on Automation and Robotics in Construction ISARC'99*. September 22-24, Madrid 1999.

[6] J. Kosecka, R. Blasi, C. J. Taylor, and J. Malik. "Vision-based lateral control of vehicles". *In Proc. Intelligent Transportation Systems Conference*, Boston, 1997.

[7] W. Leroquais, and B. D'Andra-Novel. "Transformation of the kinematic models of restricted mobility wheeled mobile robots with a single platform into chain forms". *34th Conference on Decision and Control*. New-Orleans, USA, December 1995.

[8] J. Luo and P. Tsiotras. "Control design for systems in chained form with bounded inputs". American Control Conference. Philadelphia, PA. June 24-25, 1998.

[9] M. A. Sotelo, F. J. Rodriguez, L. Magdalena, L. M. Bergasa, and L. Boquete."A Robust Vision-based Lane Tracking System for Autonomous Driving on Unmarked Roads". *Submitted to Autonomous Robots*. July 2002.

[10] H. Sussmann, E. Sontag, and Y. Yang. "A general result on the stabilization of linear systems using bounded controls". *IEEE Transactions on Automatic Control*, 39(12):2411-2425, January 1994.

[11] C. J. Taylor, J. Kosecka, R. Blasi, and J. Malik. "A comparative study of vision-based lateral control strategies for autonomous highway driving", *The International Journal of Robotic Research*. 18(5), pp. 442-453, 1999.